WALAILAK JOURNAL
http://wjst.wu.ac.th Engineering and Physical Sciences

Adsorption of Pb(II) Ions from Aqueous Solution in Fixed Bed Column by Mixture of Clay plus Bamboo Biochar

Ahmed Hassan ALAMIN[*] and Lupong KAEWSICHAN

Department of Chemical Engineering, Prince of Songkla University, Songkhla 90110, Thailand

(**[*]Corresponding author's e-mail: ahmed.10000@yahoo.com**)

Received: 14 July 2015, Revised: 16 November 2015, Accepted: 6 December 2015

Abstract

Fixed bed column experiments were conducted to investigate the adsorption potential of adsorbent mixture called CB containing Sudanese clay (CS) and bamboo biochar (BB) to form CB adsorbent for the removal of Pb(II) from aqueous solution. Characterization of CS was performed using FTIR, XRD, and XRF techniques; and, for BB, FTIR, and SEM. Effects of solution flow rate (10 - 20 ml/min), bed height (10 - 40 mm), and initial Pb(II) concentration (5 - 30 mg/L) on the breakthrough characteristics of the adsorption process were investigated. The adsorption process system was found to be better performed at low feed flow rate, low CB bed height, and high Pb(II) inlet concentration. Bed depth service time (BDST) model was used in the column performance experimental data, and model parameters were evaluated. Three other models were used to fit the adsorption data: Adams-Bohart, Thomas, and Yoon-Nelson. All models were good, but the coefficient of determination for the first and the 2 latter models were found to yield a better fit than the Adams-Bohart model and, hence, these were used to predict the adsorption of Pb(II) ions in the fixed bed column. The CB mixture was shown to be a suitable adsorbent for adsorption, or removal, of Pb(II).

Keywords: Fixed bed, clay, bamboo biochar, adsorption, Pb(II)

Introduction

Heavy metals pose an important issue in worldwide environmental problems. Effluents from a wide range of industrial applications, e.g., microelectronics, electroplating, battery manufacturing, metal finishing, mining and metallurgical products, dyestuffs, tanneries, chemicals, and pharmaceuticals, contain heavy metals and are responsible for pollution of the environment [1]. The presence of heavy metals in natural water bodies poses health problems for animals, plants, and human beings, and numerous metals such as Sb, Cr, Cd, Pb, Mn, and Hg, have toxic effects on man and environment [2]. Exposure to Pb(II), a highly toxic substance, produces a wide range of adverse health effects for both adults and children [3]. Lead poisoning causes severe damage to organs and leads to deadly diseases, thereby posing one of the greatest dangers to the living [4]. Common methods available for the removal of Pb(II) from aqueous solutions are: ion exchange, solvent extraction, membrane process, chemical precipitation, and adsorption [5], which have their advantages and disadvantages. Conventional precipitation methods do not always provide satisfactory removal rates in meeting pollution control standards, and synthetic ion-exchange resins are often expensive [6]. Adsorption is one of the most important procedures for the removal of heavy metals [7]; ion-exchange and adsorption mechanisms of various adsorbents have been used to remove a variety of heavy metal ions from aqueous solution [1].

Adsorbents such as minerals, organic materials of biological origin, zeolites, industrial by-products, agricultural wastes, biomass, and polymeric materials had been used for the removal of heavy metals from water [8]. Clays, abundant and readily available in nature, can also be used as adsorbents due to their high surface areas, chemical and mechanical stabilities, and their surface and structural properties

[9]. Many soil adsorbents have been studied for the removal of heavy metals, such as Chinese loess [10], clay [11], and bentonite [12]. In general the value of clay is in its readiness to expand and effectively increase in surface area to accommodate more metal ions [13]. Lead metal was found to be easily adsorbed onto montmorillonite, both in its raw form and its acid activated derivatives [14]. The removal of lead by Sudan clay is particularly extractive because it is a natural and local product, therefore, a cheap and easily available source; aluminosilicate [15]. Moreover, its adsorption capacity can be improved via mixing with other adsorbent, such as bamboo biochar.

Biochar, an important renewable source for securing future energy supplies from environmentally benign systems [16], is also recognized as an effective sorbent for potentially organic compounds and heavy metals [17]. Recent studies have also suggested that surface modification processes, such as growing/adding/depositing nanomaterials on biochar surfaces (biochar nanocomposites), could dramatically improve sorption ability of various water pollutants, including heavy metals, organics, phosphates, nitrates, etc. [18,19].

Preliminary investigations by the authors revealed generally higher Pb(II) adsorbing efficiencies when bamboo biochar (BB) was used as a mixture together with Sudanese clay (CS). Furthermore, there appears to be limited information on wastewater treatment using mixed adsorbents, although Pb(II) removal using such adsorbents have not been reported.

In this study, the removal efficiency of Pb(II) from aqueous solution employing a fixed bed column using a mixture of Sudan clay plus bamboo biochar was investigated. Principal design parameters: solution flow rate, column bed height, and inlet concentration of Pb(II) solution, were evaluated using a laboratory scale apparatus, and the effect of operation conditions on the removal percentage of Pb(II) was investigated.

Materials and methods

Adsorbents

Sudanese clay (CS) used in this experiment was from the Nile river region in Sennar state, Sudan. Standard metal of $Pb(No_3)_2$ was purchased from Boss Official Limited Partnership, Thailand. BB was prepared at laboratory scale by pyrolysis process at 500 °C, grinded and sieved through mesh number 20, and mixed with clay at a ratio of 1:1 to form adsorbent mixture CB. All solutions were prepared from analytical reagents (AR) and double distilled water. The mixture of adsorbents was put in circular rubber foam rings acting as holders to be fixed in a column to make a bed of varying height. Concentration of residual Pb(II) was analysed using a Perkin Elmer thermos scientific S-series model (AAnalyst100) flame atomic absorption spectrometer (AAS). Fourier transform infrared spectroscopy (FTIR) (Bomem, MB 100) was conducted to identify the functional groups of the clay and biochar. The mineralogical composition of the CS was determined using X-Ray Diffraction (XRD), and the chemical composition was determined by a Thermo ARL-9800 model X-Ray Fluorescence (XRF) spectrometer and wet analysis.

Adsorbate

Standard solution of $Pb(No_3)_2$ (1000 mg/L) was obtained by dissolving 1.59 (g) of lead nitrate in 1 litre double distilled water. Stock solutions were prepared by diluting the standard solution to various concentrations in the rage of 5 - 30 (mg/L).

Experimental setup and procedure

A schematic diagram for the fixed bed column system is shown in **Figure 1**. The column was made of a glass tube, having 35 (mm) inside diameter and 240 (mm) in height. At the bottom of the column, a stainless steel sieve was attached, followed by a layer of glass wool. A known quantity of the prepared mixture of CS and BB, to form CB, was put in the circular rubber foam ring, and was packed in the column to obtain the desired bed height of the adsorbent at ranges of 10 - 40 (mm), equivalent to 0.8 to 3.2 (g) of CB, to study the effect of bed height. The column was connected to a distributor in order to provide a uniform flow of the solution through the column. A solution of Pb(II) of known concentrations

at ranges of 5 - 30 (mg/L) was pumped downward through the column at varied flow rates at ranges of 10-20 (ml/min) controlled by a peristaltic pump to investigate the effects of initial concentration, effects of flow rate, and effects of bed height. Samples of the outlet solution were collected at the exit of the column at time intervals, and their concentrations were determined using a flame atomic adsorption spectrophotometer (AAS). In order to ensure the accuracy and reproducibility of all the data, all column adsorption experiments were conducted in triplicate, and mean values were used in the analysis.

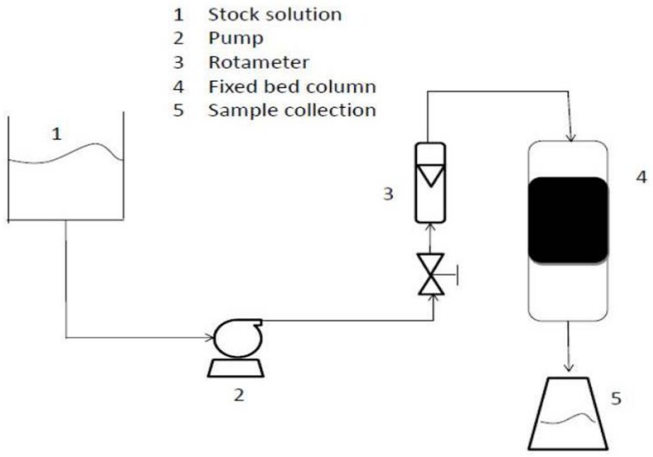

Figure 1 The fixed bed experimental setup.

Analysis of column data

Characteristics of importance in determining the operation and dynamic response of an adsorption fixed bed column are the time of breakthrough appearance and the shape of the breakthrough curve. The breakthrough curves reveal the loading behaviour of Pb(II) to be removed from the solution and is usually expressed in terms of adsorbed Pb(II) concentration (C_{ad}), inlet Pb(II) concentration (C_o), outlet Pb(II) concentration (C_t), or normalized concentration, defined as the ratio of outlet Pb(II) concentration to the inlet Pb(II) concentration (C_t/C_o), as a function of time or volume of effluent for a given bed height [20]. Effluent volume (V_{eff}) can be calculated from Eq. (1);

$$V_{eff} = Qt_{total} \quad (1)$$

where t_{total} and Q are the total flow time (min) and the volumetric flow rate (ml/min).

The area under the breakthrough curve (A), obtained by integrating the adsorbed concentration (C_{ad} in mg/L) versus t (min), can be used to find the total adsorbed Pb(II) quantity (maximum column capacity). The total adsorbed metal quantity (q_{total} in mg) in the column for a given feed concentration and flow rate (Q) can be calculated from Eq. (2);

$$q_{total} = \frac{Q\,A}{1000} = \frac{Q}{1000}\int_{t=0}^{t=t_{total}} C_{ad}\,dt \quad (2)$$

The total amount of metal ions dispatched to the column (M_{total}) can be calculated using Eq. (3);

$$M_{total} = \frac{C_0\,Qt_{total}}{1000} \quad (3)$$

The total removal is calculated from Eq. (4);

$$\text{Total removal (\%)} = \frac{q_{total}}{M_{total}} \times 100 \quad (4)$$

The equilibrium metal uptake q_{eq}, or the maximum capacity of the column, is defined by Eq. (5) as the total amount of metal sorbed q_{total} per g of adsorbent (X) at the end of the total flow time;

$$q_{eq} = \frac{q_{total}}{X} \quad (5)$$

Column breakthrough curve modelling

Successful design and operation of laboratory-scale fixed bed column adsorption can be explained by simple mathematical models. Breakthrough curves yielded for flow rate, initial concentration, and bed height were predicted by models such as bed-depth service-time (BDST), Adams-Bohart, Thomas, and Yoon-Nelson models.

The breakthrough curves using the BDST model is based on measuring the bed capacity at different percentages of breakthrough values. The model is based on an assumption that the rate of adsorption is controlled by the surface reaction between the adsorbate and the unused capacity of the adsorbent. Constants from the model can be easily scaled up for different concentrations and flow rates without conducting additional experiments. Moreover, they can be used to predict the fixed bed column performance at any bed height. The linear relationship between bed depth and service time is given by Eq. (6) [21];

$$t = \frac{NZ}{C_0 v} - \frac{1}{K_\alpha C_0} \ln\left[\left(\frac{C_0}{C}\right) - 1\right] \quad (6)$$

where C is the breakthrough Pb(II) concentration (mg/L); N the adsorption capacity of the bed (mg/L); Z the depth of the column bed (cm); v the linear flow velocity of lead solution through the bed (ml/cm^2 h); and K_α the rate constant (L/mg h).

Adams-Bohart model [22] is commonly used for description of the initial part of the breakthrough curve [23], and the model equation is expressed as Eq. (7);

$$\ln \frac{C_t}{C_0} = k_{AB} C_0 t - k_{AB} N_0 \frac{Z}{F} \quad (7)$$

where C_0 and C_t (mg/L) are the inlet and effluent Pb(II) concentration; k_{AB} (L/mg min) the kinetic constant; F (mm/min) the linear velocity calculated by dividing the flow rate by the column section area; Z (mm) the bed depth of column; and N_0 (mg/L) the saturation concentration.

One of the most popular and widely used models for describing the process theory of adsorption in a fixed bed column is the Thomas model [24]. This model assumes plug flow behaviour in the bed, and uses Langmuir isotherm for equilibrium and second-order reversible reaction kinetics. The model equation is expressed as Eq. (8);

$$\ln\left(\frac{C_0}{C_t} - 1\right) = \frac{k_{Th}\, q_0\, W}{Q} - k_{Th}\, C_0\, t \quad (8)$$

where k_{Th} (ml/min mg) is the Thomas rate constant; q_0 (mg/g) the equilibrium Pb(II) uptake per g of the adsorbent; C_o (mg/L) the inlet Pb(II) concentration; C_t (mg/L) the outlet concentration at time t; W (g) the mass of adsorbent; Q (ml/min) the flow rate; and t (min) the flow time.

Yoon and Nelson [25] had developed a model based on the assumption that the rate of decrease in the probability of adsorption of adsorbate molecule is proportional to the probability of the adsorbate adsorption and the adsorbate breakthrough on the adsorbent. The linear form of the equation is expressed as Eq. (9);

$$\ln\left(\frac{C_t}{C_0 - C_t}\right) = k_{YN}t - \tau k_{YN} \quad (9)$$

where k_{YN} (min^{-1}) is the Yoon-Nelson proportionality constant; and τ (min) the time required for retaining 50 % of the initial sorbate.

Results and discussion

Characteristics of the Sudanese clay

FTIR spectrum curves for the clay sample in **Figure 2** shows changes in the functional groups which can be observed in all frequency ranges. The spectrum of the clay exhibits a broad shoulder at around 3700 - 3400 cm^{-1}; the range of frequencies usually assigned to surface hydroxyl groups and sorbed water. The absorption band observed at 3622 cm^{-1} for clay is attributable to hydroxyl group vibrations in Mg-OH-Al, Al-OH-Al, and Fe-OH-Al units in the octahedral layer. This poorly resolved shoulder consists of overlaps of 2 components: Si-OH at 3622 cm^{-1} and Mg-OH at 3697 cm^{-1} stretching vibrations. The band at 3448 cm^{-1} is due to the O-H stretching vibration of the silanol Si-OH groups and HO-H vibration of the water adsorbed by the silica surface. The spectrum also contains a broad band at 1457 cm^{-1} related to the stretch vibrations of C=O group due to calcite impurity. The broad band near 1034 cm^{-1} is related to the stretch vibrations of the Si-O groups. The band appearing at 1457 cm^{-1} corresponds to that of carbonate [calcite ($CaCO_3$) or dolomite (Ca, $Mg(CO_3)_2$)]. In the low energy region, the spectrum shows one band around 685 cm^{-1} due to O–H bending vibration from the adsorbed water, and one band at 535 cm^{-1} assigned to Mg-O vibration. The bands appearing at 468 cm^{-1} correspond to SiO Mg.

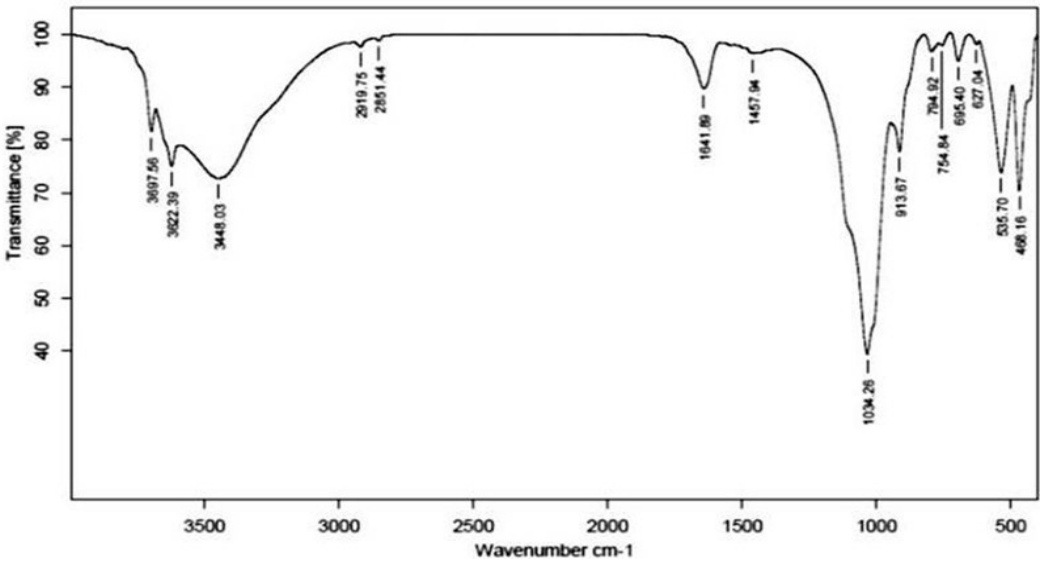

Figure 2 FTIR Analysis of the Sudanese clay.

XRD measurements show that the Sudanese clay is mainly composed of (Albite, calcian, ordered), besides quartz, kaolinite, and montmorillonite; significant peaks are identified on the XRD spectrum in **Figure 3**. Chemical compositions of the clay are tabulated in **Table 1**.

SEM for bamboo biochar and clay:

The BB morphological characteristics obtained by SEM showed a large internal surface and porous structure with an approximate porous space of 38.67 µm, as shown in **Figures 4(a)** and **4(b)** with different magnitudes. Furthermore, SEM of elemental composition in the BB sample is shown in **Table 2**.

The SEM analysis of clay was investigated to study the surface, as shown in **Figures 4(c)** and **4(d)**. It is revealed clearly from the image that the surface is porous. In general, porous materials act as adsorbents.

Characteristics of the bamboo biochar

FTIR spectrum analysis of the bamboo biochar sample (figure not shown) revealed many functional groups on its surfaces: the bands assigned to O–H stretching; aliphatic C-H stretching; intense bands of aliphatic CH_2; intensity of aromatic C=C stretching and C=O stretching of conjugated ketones and quinones; C=C ring stretching vibration of lignin; and C–O and C–C stretching.

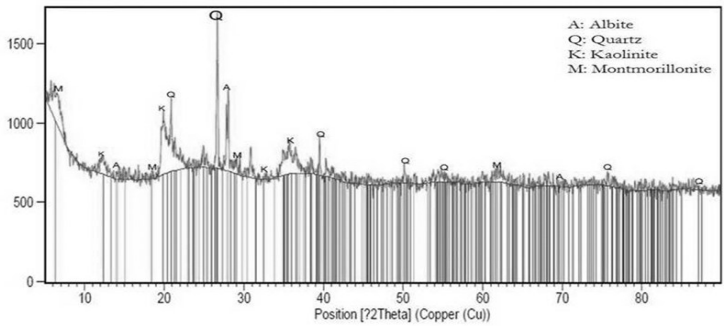

Figure 3 XRD Chart on the Sudanese clay.

Table 1 Characteristics of the Sudanese clay

Chemical composition of the clay (%)	
Na_2O	1.437
MgO	2.106
Al_2O_3	20.637
SiO_2	47.612
K_2O	0.310
CaO	1.972
TiO_2	1.393
MnO	0.159
Fe_2O_3	11.219
SrO	0.015
ZrO_2	0.023
Others	13.117
Other parameters:	
Organic matters	12.82±0.44 g/kg
pH	9.98±0.01
Conductivity	514±3.06 µS/cm
Particle size	139.4 µm
Density	2.275±0.003 g/cm^3

Table 2 Characteristics of the bamboo biochar

Chemical composition of the bamboo biochar (%)	
C	58.61
K	30.46
Cl	9.38
S	1.55
Other Parameters:	
pH	8.000±0.001
Density	0.394±0.005 g/cm^3

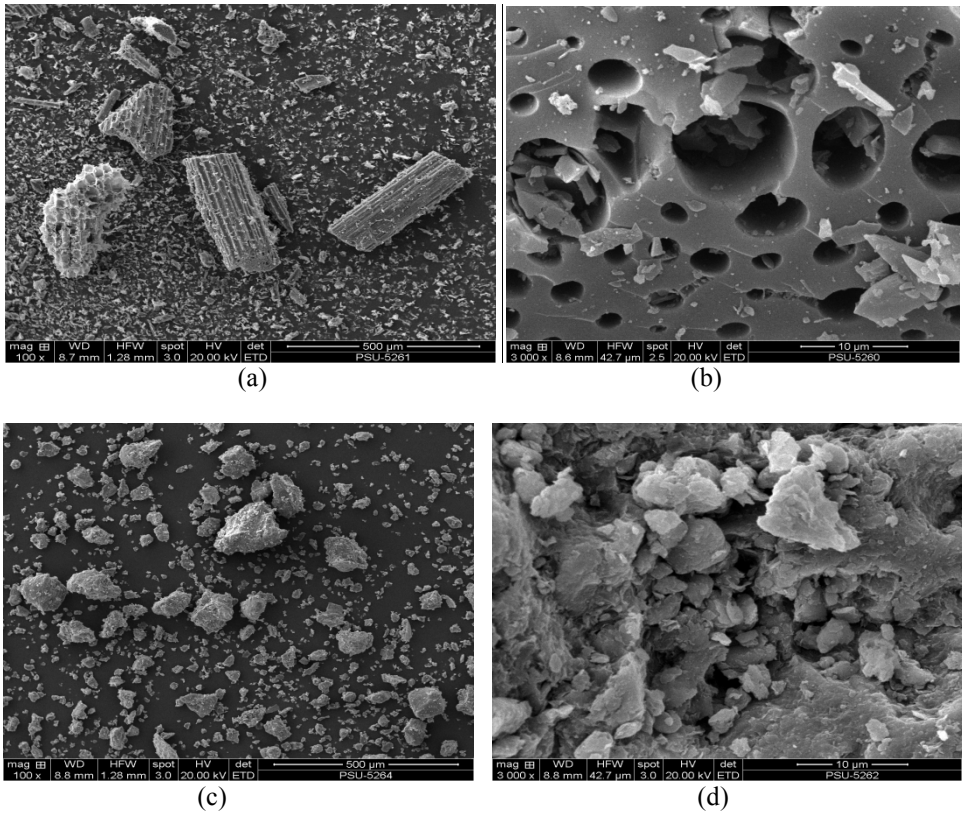

Figure 4 SEM of the bamboo biochar [(a) and (b)], and of the clay adsorbent [(c) and (d)].

Effect of Pb(II) solution flow rate

The effect of flow rate on adsorption of Pb(II) using the CB adsorbent was investigated under various flow rates in the range of 10 - 20 ml/min, whilst other variables were fixed (adsorbent bed height of 25 (mm) and an inlet Pb(II) concentration of 17.5 (mg/L)). Breakthrough curves obtained are shown in **Figure 5**. Generally, the breakthrough occurred slower with lower flow rate. Similarly, the breakthrough time to reach saturation decreased significantly with increasing flow rate. The curves represented at high

flow rate were much sharper those that in the case of low flow rate. This can be explained by the fact that at low flow rate the residence time of Pb(II) ions in the column increases, hence, the Pb(II) ions have more time to diffuse into the pores of the CB through intraparticle diffusion, resulting in a longer breakthrough time and saturation time [26].

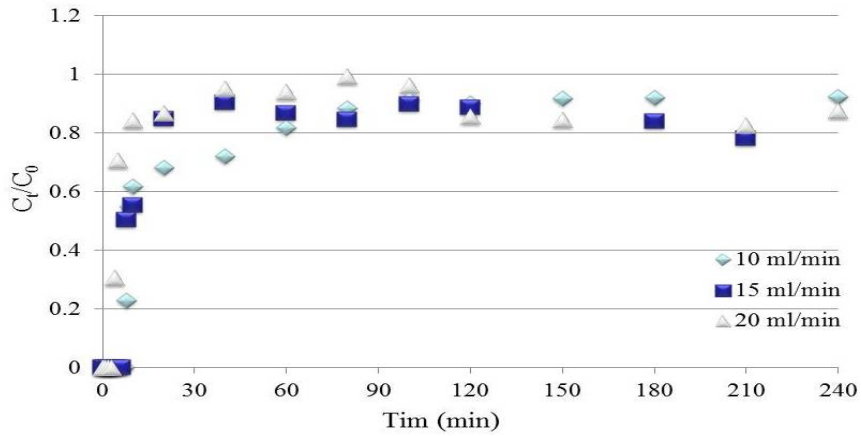

Figure 5 Breakthrough curves for Pb(II) adsorption on the CB at different flow rate (at constant inlet Pb(II) concentration of 17.5 (mg/L) and bed height of 25 (mm)).

Effect of initial Pb(II) concentration

The effect of initial metal concentration on adsorption of Pb(II) by the CB adsorbent were investigated using different inlet Pb(II) concentrations in the range of 5 - 30 (mg/L) while other parameters were kept constant (adsorbent bed height of 25 (mm) and solution flow rate of 15 (ml/min)). **Figure 6** shows the breakthrough curves obtained from various concentration of Pb(II). From the adsorption data, the breakthrough time, the removal efficiency, and the saturation time decreased with the increase in initial concentration of the Pb(II) ions. The diffusion happens when there is a concentration gradient, diffusion will normally proceed from an area of higher concentration to an area of lower concentration, and at the end of the time equilibrium will occur. There are several factors affecting the rate of diffusion; one of these being concentration of the solution. The major difference in concentration would be a more rapid rate of diffusion. The second factor is the mass of the molecules diffusing; heavier molecules move more slowly, therefore, they diffuse more slowly, and the reverse is true for lighter molecules. This can be explained by the fact that a lower concentration causes a slower transport due to the decrease in the diffusion coefficient or mass transfer coefficient [23]. The Pb(II) ions adsorbed into the CB adsorbent increased from 306 to 887 and 905 (mg), respectively, with the inlet initial concentration of 5, 17.5 and 30 (mg/L). The increase in inlet concentration of Pb(II) ions has an effect on the metal uptake capacity of the CB due to saturation of the column. The increase in the Pb(II) uptake capacity of the CB is due to the fact that a higher inlet concentration provides a higher driving force for the transfer process in order to overcome the mass transfer resistance [27].

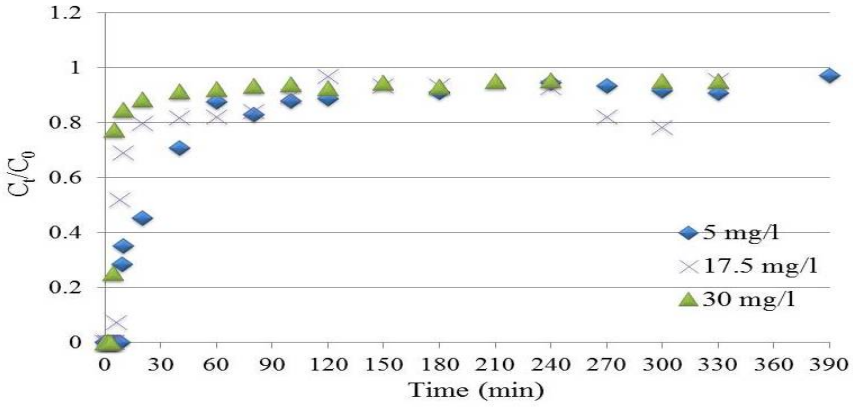

Figure 6 Breakthrough curves for Pb(II) adsorption on the CB at different inlet Pb(II) concentrations (at constant bed height of 25 (mm) and flow rate of 15 (ml/min)).

Effect of adsorbent bed height

Removal of Pb(II) in the adsorption process using CB adsorbent was studied under the effect of bed height while flow rate and inlet concentration of Pb(II) were kept constant, at 15 (ml/min) and 17.5 (mg/L), respectively. The breakthrough curves for bed heights of 10, 25, and 40 (mm) are shown in **Figure 7**. The breakthrough curves obtained were steeper with lower bed height. When bed height increased, the removal efficiency, the breakthrough time, and the saturation time increased. This increase in removal efficiency of Pb(II) ions into the CB adsorbent is due to the higher number of adsorption sites available and the increase in volume influent. The slope of the breakthrough curve decreased with increasing bed height, resulting in a broadened mass transfer zone [23]. The highest adsorption capacity was observed at the highest bed height due to an increase in the surface area of adsorbent, which provided more binding sites for the adsorption [28].

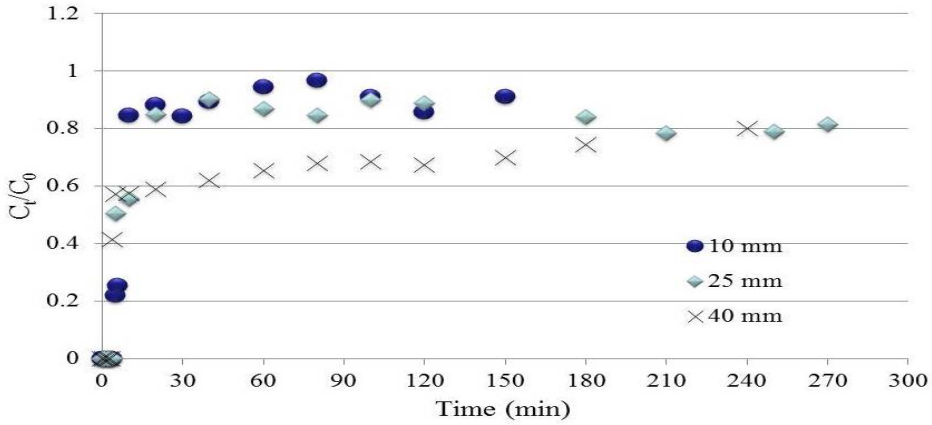

Figure 7 Breakthrough curves for Pb(II) adsorption on the CB at different bed heights (at constant inlet Pb(II) concentration of 17.5 (mg/L) and flow rate of 15 (ml/min)).

Dynamic adsorption models employed

Variables from the breakthrough curves can be used to predict the design column efficiency. The four mathematical models used here to predict the efficiency of the laboratory-scale column and its dynamic behaviour are: the bed-depth service time (BDST), the Adams-Bohart, the Thomas, and the Yoon-Nelson models.

The bed depth service time (BDST) model

The BDST model plot of service time versus bed depth at flow rate of 15 ml/min is linear, as shown in **Figure 8**. The correlation coefficient value R^2 of 0.9959 is very high, pointing to very good validity of the model. The calculated values of the model parameters (N) and (K_α) are 393.75 (mg/L) and 0.037 (L/mg h), respectively. In the case of large (K_α) value, a short bed is enough to avoid breakthrough, but as (K_α) gets smaller, as in this study, a progressively deeper bed is required to avoid breakthrough [29].

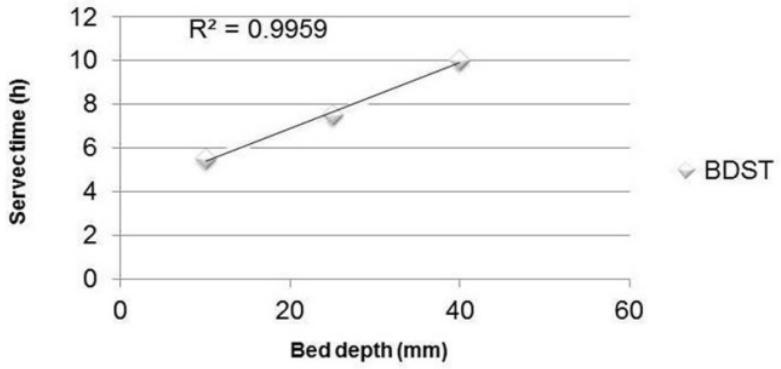

Figure 8 BDST plot for Pb(II) adsorption on CB.

The Adams-Bohart model

The Adams-Bohart model was applied to the experimental data, and the value of adsorption capacity for adsorbent (N_0) and the kinetic constant of the model (k_{AB}) were calculated and presented in **Table 3**, together with the correlation coefficients (obtained in range of 0.9182 to 0.9788). According to this model, the equilibrium is not instantaneous, and the rate of sorption Pb(II) on CB adsorbent is proportional to the fraction of sorption capacity [27]. Although the Adams-Bohart model gives a simple and comprehensive approach for evaluating column dynamics, its validity in the adsorption process of Pb(II) by CB is limited to the range of conditions used [30]. From the table, (N_0) increased with increasing inlet concentration of Pb(II) and the flow rate, whereas the trend for (k_{AB}) was the opposite, indicating that the overall system kinetics were dominated by external mass transfer in the initial part of adsorption in the column [31]. In bed height parameter, (N_0) increased with increasing bed height, while (k_{AB}) decreased.

The Thomas model

The experimental data were fitted to the Thomas model. The calculated rate constant (k_{Th}), the maximum sorption capacity (q_0), and the correlation R^2 (obtained in range of 0.8839 to 0.9838) are listed in **Table 4**. From the table, k_{Th} decreased with increasing inlet concentration of Pb(II) due to the increase in mass transport resistance while the values of (q_0) were increasing. This is attributable to the driving force of adsorption for the difference in concentrations between Pb(II) on the CB adsorbent surface and in the solution [32]. Thus, the higher driving force due to the higher lead concentration resulted in larger q_0

[33]. The maximum sorption capacity q_0 decreases with increasing bed height and flow rate. That means q_0, affected by increase in CB mass, is due to more adsorption sites being available for Pb(II) ions as the amount of CB increased. At lower flow rates, there is a longer contact time between the Pb(II) ions and CB adsorbent and, therefore, a higher value of the rate constant, suggesting that the adsorption capacity will reach the equilibrium value faster [34]. The rate constant of the Thomas model k_{Th} also decreased with increasing bed height. It was demonstrated that Pb(II) adsorption into CB followed pseudo-second order reaction, and both external and intraparticle diffusion were involved in the adsorption process. These mean that the Thomas model was suitable for adsorption processes where external and internal diffusions were not the limiting step [35].

The Yoon-Nelson model

The fourth and final model applied to the experimental data is the Yoon-Nelson model. The Yoon-Nelson proportionality constant (k_{YN}) and the time required for retaining 50 % (τ) calculated for all data of the breakthrough curves with corresponding correlation coefficient are shown in **Table 5**. The range of R^2 between 0.9287 and 0.9904 obtained from this model represents a better fit than the Adams-Bohart and the Thomas model, but not the BDST model. The rate constant significantly increases with increase in flow rate and decreases with increase in bed height. In the case of high flow rate the number of Pb(II) molecules passing through a particular CB adsorbent was more, which increases the rate. Also, at higher bed height, the Pb(II) molecules have more time to immigrate through the column, which results in the reduced adsorption rate [36]. The time retaining 50 % (τ) was found to significantly decrease with the increase in inlet Pb(II) concentration and the flow rate of the solution. This is due to the fact that saturation of the column was rapidly achieved, while τ increased with the increase in bed height because saturation was slower at thicker bed height.

Table 3 Adams-Bohart model result from linear regression analysis

Initial concentration (mg/L)	Flow rate (ml/min)	Bed height (mm)	k_{AB} (L/mg min)	N_0 (mg/L)	R^2
5	15	25	0.0024	298.26	0.9267
17.5	15	25	0.000262857	939.68	0.9263
30	15	25	0.0002	1090.66	0.9544
17.5	10	25	0.000297143	891.63	0.9788
17.5	15	25	0.0002	1090.66	0.9544
17.5	20	25	0.000182857	1283.8	0.9506
17.5	15	10	0.000411429	478.81	0.9182
17.5	15	25	0.000262857	939.68	0.9263
17.5	15	40	6.28571E-05	2827.58	0.9501

Table 4 Thomas model result from linear regression analysis.

Inlet concentration (mg/L)	Flow rate (ml/min)	Bed height (mm)	k_{Th} (L/mg min)	q_0 (mg/g)	R^2
5	15	25	0.003780000	7352.58	0.8839
17.5	15	25	0.000542857	9319.21	0.9763
30	15	25	0.000610000	12313.52	0.9795
17.5	10	25	0.000577143	18018.94	0.9552
17.5	15	25	0.002834286	9852.22	0.8841
17.5	20	25	0.000542857	9319.21	0.9763
17.5	15	10	0.000942857	25444.60	0.9832
17.5	15	25	0.000577143	18018.94	0.9552
17.5	15	40	0.000377143	2682.20	0.9586

Table 5 Yoon-Nelson model result from linear regression analysis.

Inlet concentration (mg/L)	Flow rate (ml/min)	Bed height (mm)	k_{YN} (L/mg min)	τ (min)	R^2
5	15	25	0.0196	221.62	0.9670
17.5	15	25	0.0124	197.84	0.9849
30	15	25	0.0183	54.73	0.9795
17.5	10	25	0.0101	205.93	0.9552
17.5	15	25	0.0124	197.84	0.9849
17.5	20	25	0.0101	67.73	0.9904
17.5	15	10	0.0165	77.55	0.9832
17.5	15	25	0.0124	197.84	0.9849
17.5	15	40	0.0028	123.11	0.9900

Conclusions

Clay and bamboo biochar are capable of being used in the treatment for the removal of heavy metal from aqueous solution, particularly when the mixed together. CB, a mixture of Sudanese clay plus bamboo biochar (a low cost material), was employed as an adsorbent for removal of Pb(II) ions from aqueous solution in a fixed bed column. The varying variables investigated were: initial inlet ion concentration, flow rate, and bed height. The system was found to better perform at low feed flow rate, low CB bed height, and high Pb(II) inlet concentration. The BDST model was used in the column performance experimental data,, and model variables were calculated. The column data obtained fitted well with 3 other mathematical models: the Adams-Bohart, the Thomas and the Yoon-Nelson models. All models can be applicable, but the first and latter 2 models, the BDST, the Thomas and Yoon-Nelson, were found to better predict the breakthrough curves than the Adams-Bohart. This work shows that CB adsorbent can play an important role in the adsorption of Pb(II) from water in a column. Taking its low cost into consideration, CB could be regarded as a new, moderately effective adsorbent that can be applied in the field of industrial wastewater treatment.

Acknowledgements

The authors are grateful to the Prince of Songkla University (PSU) for their financial assistance and support for this research. We would also like to thank the PSU Department of Chemical Engineering and the Discipline of Excellence (DoE) in Chemical Engineering for assistance in carrying out the needed chemical analyses.

References

[1] SH Lin, SL Lai and HG Leu. Removal of heavy metals from aqueous solution by chelating resin in a multistage adsorption process. *J. Hazard. Mater*. 2000; **76**, 139-53.

[2] VCT-Costodes, H Fauduet, C Porte and A Delacroix. Removal of Cd(II) and Pb(II) ions, from aqueous solutions, by adsorption onto sawdust of *Pinus sylvestris. J. Hazard. Mater*. 2003; **105**, 121-42.

[3] AA Farghali, M Bahgat, A E-Allah and MH Khedr. Adsorption of Pb(II) ions from aqueous solutions using copper oxide nanostructures. *Beni-Suef Univ. J. Basic Appl. Sci*. 2013; **2**, 61-71.

[4] V Singh, S Tiwari, AK Sharma and R Sanghi. Removal of lead from aqueous solutions using *Cassia grandis* seed gum-graft-Poly(methylmethacrylate). *J. Colloid Interface Sci*. 2007; **316**, 224-32.

[5] MM Kumar. Removal of Pb(II) from aqueous solution by adsorption using activated tea waste. *Korean J. Chem. Eng*. 2010; **90**, 3266-71.

[6] CW Chung and FT Ping. Adsorption/ion-exchange Behavior between a water-insoluble cationic starch and 2-Chlorophenol in aqueous solutions. *J. Appl. Polym. Sci*. 1998; **67**, 1085-92.

[7] A Sarı, M Tuzen, D Cıtak and M Soylak. Adsorption characteristics of Cu(II) and Pb(II) onto expanded perlite from aqueous solution. *J. Hazard. Mater*. 2007; **148**, 387-94.

[8] TA Kurniawan, GYS Chan, W Lo and S Babel. Comparisons of low-cost adsorbents for treating wastewaters laden with heavy metals. *Sci. Total Environ*. 2006; **366**, 409-26.

[9] P Liu. Polymer modified clay minerals: A review. *Appl. Clay Sci*. 2007; **38**, 64-76.

[10] X Tang, Z Li, Y Chen and Z Wang. Removal of Zn(II) from aqueous solution with natural Chinese loess: Behaviors and affecting factors. *Desalination* 2009; **249**, 49-57.

[11] JUK Oubagaranadin and ZVP Murthy. Adsorption of divalent lead on a montmorillonite- illite type of clay. *Ind. Eng. Chem. Res*. 2009; **48**, 10627-36.

[12] A Mellah and S Chegrouche. The removal of Zinc from aqueous solutions by natural bentonite. *Water Res*. 1997; **31**, 621-9.

[13] MEI Ahmed. Selective adsorption of cadmium species onto organic clay using experimental and geochemical speciation modeling data. *Int. J. Eng. Tech*. 2016; **8**, 128-31.
[14] KG Bhattacharyya and SS Gupta. Pb(II) uptake by kaolinite and montmorillonite in aqueous medium: Influence of acid activation of the clays. *Colloids Surface A* 2006; **277**, 191-200.
[15] MA Ismail, MAZ Eltayeb and SA Maged. Elimination of heavy metals from aqueous solutions using Zeolite LTA synthesized from sudanese clay. *Res. J. Chem. Sci*. 2013; **3**, 93-8.
[16] Y Yu and H Wu. Bioslurry as a Fuel. 2. Life-cycle energy and carbon footprints of bioslurry fuels from Mallee Biomass in Western Australia. *Energ. Fuel* 2010; **24**, 5660-8.
[17] CT Chiou and DE Kile. Deviations from sorption linearity on soils of polar and nonpolar organic compounds at low relative concentrations. *Environ. Sci. Tech*. 1998; 1998; **32**, 338-43.
[18] M Zhang, B Gao, Y Yao, Y Xue and M Inyang. Synthesis of porous MgO-biochar nanocomposites for removal of phosphate and nitrate from aqueous solutions. *Chem. Eng. J*. 2012; **210**, 26-32.
[19] M Inyang, B Gao, Y Yao, Y Xue, AR Zimmerman, P Pullammanappallil and X Cao. Removal of heavy metals from aqueous solution by biochars derived from anaerobically digested biomass. *Bioresour. Tech*. 2012; **110**, 50-6.
[20] J Guo and AC Lua. Textural and chemical properties of adsorbent prepared from palm shell by phosphoric acid activation. *Mater. Chem. Phys*. 2003; **80**, 114-9.
[21] RA Hutchins. New methods simplifies design of activated carbon system. *Chem. Eng*. 1973; **80**, 133-8.
[22] GS Bohart and EQ Adams. Some aspects of the behavior of charcoal with respect to chlorine. *J. Am. Chem. Soc*. 1920; **42**, 523-44.
[23] AA Ahmad and BH Hameed. Fixed-bed adsorption of reactive azo dye onto granular activated carbon prepared from waste. *J. Hazard. Mater*. 2010; **175**, 298-303.
[24] HC Thomas. Heterogeneous ion exchange in a flowing system. *J. Am. Chem. Soc*. 1944; **66**, 1664-6.
[25] YH Yoon and JH Nelson. Application of gas adsorption kinetics. Part 1. A Theoretical model for respirator cartridge service time. *Am. Ind. Hyg. Assoc. J*. 1984; **45**, 509-16.
[26] G Yan and T Viraraghavan. Heavy metal removal in a biosorption column by immobilized *M. rouxii* biomass. *Bioresour. Tech*. 2001; **78**, 243-9.
[27] R Lakshmipathy and NC Sarada. A fixed bed column study for the removal of Pb^{2+} ions by watermelon rind. *Environ. Sci. Water Res. Tech*. 2015; **1**, 244-50.
[28] Z Zulfadhly, MD Mashitah and S Bhatia. Heavy metals removal in fixed-bed column by the macro fungus *Pycnoporus sanguineus*. *Environ. Pollut*. 2001; **112**, 463-70.
[29] I Mobasherpour, E Salahi and A Asjodi. Research on the batch and fixed-bed column performance of red mud adsorbents for Lead removal. *Can. Chem. Trans.* 2014; **2**, 83-96.
[30] ZZ Chowdhury, SM Zain, AK Rashid, RF Rafique and K Khalid. Breakthrough curve analysis for column dynamics sorption of Mn(II) ions from wastewater by using *Mangostana garcinia* peel-based granular-activated carbon. *J. Chem*. 2013; **2013**, 959761.
[31] R Han, L Zou, X Zhao, Y Xu, F Xu, Y Li and Y Wang. Characterization and properties of iron oxide-coated zeolite as adsorbent for removal of copper(II) from solution in fixed bed column. *Chem. Eng. J*. 2009; **149**, 123-31.
[32] Z Aksu and F Gönen. Biosorption of phenol by immobilized activated sludge in a continuous packed bed: Prediction of breakthrough curves. *Process Biochem*. 2004; **39**, 599-613.
[33] EI Unuabonah, MI El-Khaiary, BI Olu-Owolabi and KO Adebowale. Predicting the dynamics and performance of a polymer-clay based composite in a fixed bed system for the removal of lead (II) ion. *Chem. Eng. Res. Des.* 2012; **90**, 1105-15.

[34] AB Albadarin, C Mangwandi, AH Al-Muhtaseb, GM Walker, SJ Allen and MNM Ahmad. Modelling and fixed bed column adsorption of Cr(VI) onto orthophosphoric acid-activated lignin. *Chin. J. Chem. Eng.* 2012; **20**, 469-77.
[35] SS Baral, N Das, TS Ramulu, SK Sahoo, SN Das and GR Chaudhury. Removal of Cr(VI) by thermally activated weed *Salvinia cucullata* in a fixed-bed column. *J. Hazard. Mater*. 2009; **161**, 1427-35.
[36] P Sivakumar and PN Palanisamy. Packed bed column studies for the removal of Acid blue 92 and Basic red 29 using non-conventional adsorbent. *Indian J. Chem. Tech*. 2009; **16**, 301-7.